On Transport in Vertical Graphene Heterostructures

Qin Zhang, *Member, IEEE*, Gianluca Fiori, *Member, IEEE*, and Giuseppe Iannaccone, *Senior Member, IEEE*

***Abstract*— We investigate charge transport through a vertical semiconductor-graphene-semiconductor heterostructure with quantum simulations using an atomistic tight-binding Hamiltonian within the nonequilibrium Green's function formalism. We show that the normal transmission coefficient and therefore the current through the heterostructure can be greatly influenced by the atomically thin graphene layer, depending on the coupling between layers and on the k-space transmission overlap between graphene and the semiconductor. Our insights enable better understanding of transport through vertical heterostructure and highlight design parameters that might be used for the optimization of graphene-based heterostructure devices exploiting off-plane transport.**

***Index Terms*— Graphene, graphene-based heterostructures, graphene-base transistor, NEGF simulation.**

I. Introduction

SINCE the discovery of graphene in 2004 [1], its high mobility and one-atom-thin thickness has made it an attractive electronic material for radio frequency (RF) applications. Graphene field-effect transistors (GFETs) have been demonstrated with a cut-off frequency of few hundred gigahertz [2]–[4], but the lack of bandgap fundamentally limits the device current ON/OFF ratio (<10) and the power gain. Alternatively, graphene devices based on off-plane (i.e., vertical) transport, have been proposed [5]–[8], exhibiting high current ON/OFF ratios of $\sim 10^4 - 10^5$ in experiments [9]–[11]. Graphene base transistor (GBT) [7], [8], [10]–[13], is one of the vertical transistors where the one-atom-thin graphene layer (base) is sandwiched between insulating or semiconducting layers (emitter and collector). Similar to hot electron transistors, the carrier injection in GBT is controlled by the emitter-base voltage through modulating the potential barrier, while the base transit time and series resistance are expected to benefit from graphene's unique properties: ultrathin and highly conductive. Experimentally, however, the ON-state current and the common-base current gain are not as promising as projected in simulations where graphene is treated semiclassically as an ultrathin barrier [7]. In addition, it has also been experimentally observed that single-layer graphene is not transparent to low-energy transmission electron beams, showing 27% opacity [14]. As important and pressing to fully understand transport through a vertical semiconductor-graphene-semiconductor heterostructure, in order to improve the performance of GBTs [10]–[13], and to further explore devices based on off-plane transport in graphene and two-dimensional materials.

In this work, we investigate transport across the vertical semiconductor-graphene-semiconductor (SGS) heterostructure by atomistic tight-binding simulations, considering several semiconductor materials (GaAs, GaN and Si). We show that graphene layer cannot be simply treated as a transparent barrier. The normal transmission coefficient can be greatly influenced by the coupling between graphene and the semiconductor layers, and also by the overlap between their energy-dispersion relationship in the k-space.

II. Simulation Approach

The simulated vertical heterostructure is depicted in Fig. 1(a) and (b). The semiconductors are represented in a pseudo cubic structure, where the lattice constant is $1.5a$ in the x direction and $\sqrt{3}a$ in the y direction, $a = 1.42$ Å is the carbon-carbon bond length. The use of a simplified pseudo-crystal for the semiconductor allows us to consider the system at a higher abstraction level, neglecting the complexity arising from lattice mismatch between graphene and the semiconductors, and the issues related with lattice alignment and orientation. The Hamiltonian for the semiconductor is constructed with the tight-binding hopping matrix elements s_x, s_y, and the transmission coefficient is calculated as a function of energy and wave vector k_x ($k_y = 0$) or k_y ($k_x = 0$). The conduction band (CB) and valence band (VB) are then obtained with transmission coefficient $= 1$ above the CB and below the VB, and transmission coefficient $= 0$ between the CB and VB, so that s_x, s_y are extracted to fit the semiconductor's energy dispersion in both k_x and k_y directions near the CB minimum and VB maximum with the effective mass approximation. In this way, the semiconductor is described with a two-band effective mass Hamiltonian, and the atomistic interaction between graphene and the semiconductor can be built with minimized Hamiltonian matrix size. This method can also be applied to dielectrics, and be implemented into device simulation [6] for dielectric/graphene/dielectric structures. The carbon-carbon hopping parameter in graphene is $\gamma_0 = -2.7$ eV [15]. The simulated unit cell consists of two semiconductor atoms and four graphene atoms, shown in Fig. 1(b), where one semiconductor atom interacts with two nearest neighbor carbon atoms by means of the hopping parameter t_1, and the other with six nearest-neighbor carbon

Manuscript received June 11, 2014; accepted June 24, 2014. Date of publication July 31, 2014; date of current version August 21, 2014. This work was supported by the European Commission through the FP7 STREP Project GRADE under Grant 317839 awarded to IU.NET. The review of this letter was arranged by Editor E. A. Gutiérrez-D.

The authors are with "Dipartimento di Ingegneria dell'Informazione" and SEED-PUSL, University of Pisa, Italy (e-mail: qinz2008@gmail.com).

Color versions of one or more of the figures in this letter are available online at http://ieeexplore.ieee.org.

Digital Object Identifier 10.1109/LED.2014.2334052

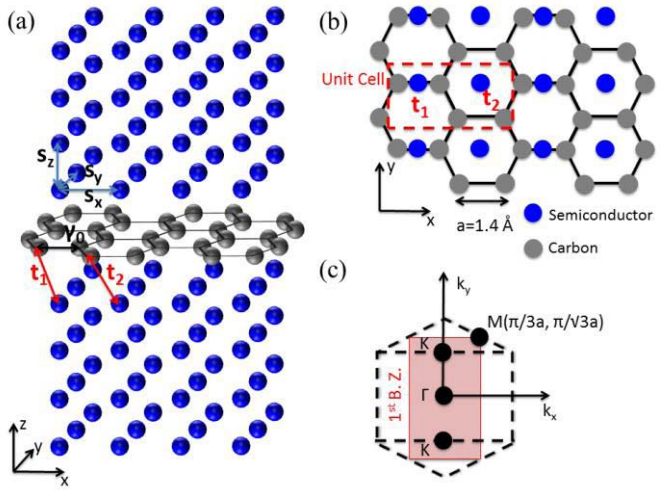

Fig. 1. (a) Vertical semiconductor-graphene-semiconductor heterostructure with pseudo semiconductor atoms (blue) and carbon atoms (grey). The blue arrows denote the inter-atomic tight-binding hopping matrix elements s_x, s_y, s_z in the semiconductor, and the red arrows denote the hopping parameters t_1, t_2 between the semiconductor and graphene. $\gamma_0 = -2.7$ eV is the carbon-carbon hopping parameter in graphene. (b) Top view of the structure with a unit cell consisting of four carbon atoms and two pseudo semiconductor atoms. (c) The first Brillouin Zone (B.Z., red) with high symmetry points Γ, K, and M.

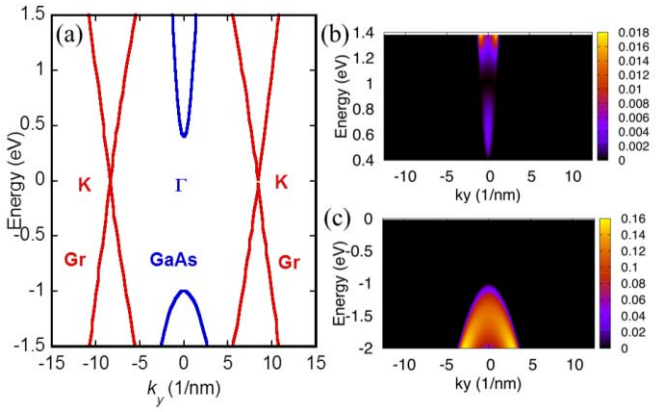

Fig. 2. (a) Energy dispersion along the k_y direction for graphene (tight-binding, red) and GaAs (100) (2-band effective mass approximation, blue), for $k_x = 0$ and $k_z = 0$. (b) Contour plot of conduction band and (c) valence band transmission coefficient through the vertical GaAs-graphene-GaAs heterostructure, with $t_1 = -0.3$ eV and $t_2 = -0.2$ eV, for $k_x = 0$.

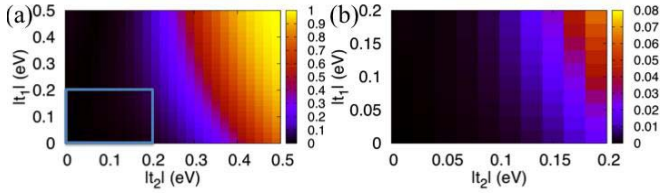

Fig. 3. (a) Transmission coefficient for the vertical GaAs-graphene-GaAs heterostructure at Γ point and 0.3 eV below the valence band maximum, as a function of semiconductor-graphene coupling strength, the absolute value of t_1 and t_2. (b) The zoom-in view of the blue rectangle in (a).

atoms with the hopping parameter t_2 [16]. Using this new basis, the first Brillouin Zone (BZ) is constructed and shown in Fig. 1(c), referenced to the regular hexagonal BZ for graphene (dashed line) with two carbon atoms in the unit cell. The high symmetry points K, where the "zero gap" of graphene is located, are refolded into the new BZ with $k_x = 0$ and $k_y = \pm 2\pi/3\sqrt{3}a$/nm.

In the tight-binding Hamiltonian matrix of the heterostructure an effective potential is included to take account for the band offset between the graphene work function [17] and the semiconductor electron affinity [18]. Non-Equilibrium Green's function (NEGF) formalism is used to simulate the ballistic transport across the vertical SGS heterostructure, exploiting the NanoTCAD ViDES simulation environment [19], [20].

III. Results and Discussions

Although graphene behaves like a "zero gap" semi-metal in lateral GFETs, it actually has a large gap at the Γ point in the vertical transport. As a guide to the eye, and to qualitatively understand mismatch between the two materials, in Fig. 2 (a) the energy dispersion for graphene and GaAs (100) are plotted along the k_y direction, for $k_x = 0$ and $k_z = 0$. The large band gap (∼5.4 eV) of graphene at Γ point is expected to be a large barrier for electrons/holes in direct semiconductors (i.e. 2.3/1.7 eV for GaAs) attempting to tunnel through, which is confirmed by simulations of vertical transport across the GaAs-graphene-GaAs heterostructure, with the graphene-GaAs coupling parameters $t_1 = -0.3$ eV and $t_2 = -0.2$ eV. The contour plot of the transmission coefficients is shown in Fig. 2(b), where the band curvature of GaAs is maintained. However, the transmission is severely suppressed, especially for the electrons, down to units of 10^{-3}. Transmission of holes is relatively higher because the barrier represented by graphene at the Γ point is lower for holes than for electrons, and electrons in GaAs have smaller effective mass than holes (Fig. 2(a)).

Without information from *ab* initio calculations, the hopping parameters between graphene and the semiconductor - t_1 and t_2 - are two unknown variables in the Hamiltonian matrix. The dependence of transmission coefficients on the coupling strength is simulated near the valence band maximum (0.3 eV below) for GaAs-graphene-GaAs heterostructure, and plotted in Fig. 3. It is shown that the transmission is strongly dependent on the coupling: with a strong coupling, the transmission across the heterostructure can reach unity, meaning that the graphene layer is effectively transparent; while a weak coupling can degrade the transmission by several orders of magnitude.

To increase the ON-state current in GBTs, it is necessary to have a large transmission through the vertical heterostructure. Other than improving the coupling between the graphene base layer and the semiconductor emitter/collector, it is also helpful to choose, for the emitter and collector, semiconducting materials that have larger transmission overlaps with graphene. Since graphene's work function is ∼4.5 eV [17], closer to most semiconductor's conduction band minimum [18], a wide bandgap semiconductor has more transmission overlap with graphene in the valence band. For example,

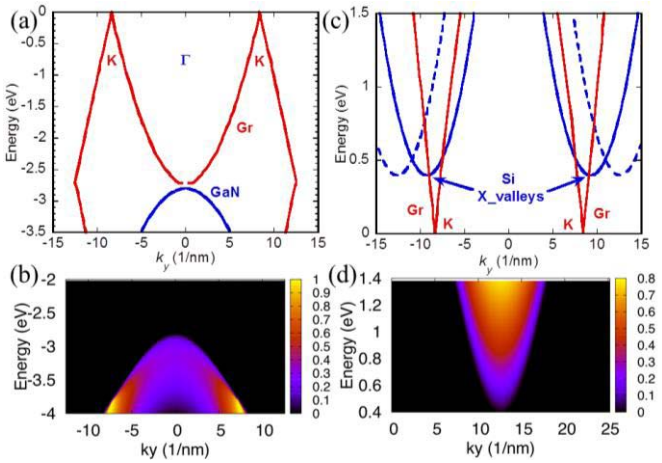

Fig. 4. (a) Valence band dispersion along the k_y direction for graphene (tight-binding, red) and zinc-blende GaN (100) (2-band effective mass approximation, blue) for $k_x = 0$ and $k_z = 0$. (b) Transmission coefficient through the valence band of the vertical GaN-graphene-GaN heterostructure, with $t_1 = -0.3$ eV and $t_2 = -0.2$ eV, for $k_x = 0$. (c) Conduction band dispersion along the k_y direction for graphene (tight-binding, red) and Si (2-band effective mass approximation, blue solid). The blue dashed line is applied in the model for simplicity. (d) Transmission coefficient through the conduction band of the vertical Si-graphene-Si heterostructure, with $t_1 = -0.3$ eV and $t_2 = -0.2$ eV, for $k_x = 0$.

Fig. 4(a) shows the valence band dispersion for zinc-blende GaN (100) and graphene along the k_y direction, where the GaN valence band maximum is below the graphene bandgap at Γ point. The transmission through the valence band of the vertical GaN-graphene-GaN heterostructure is plotted in Fig. 4(b) with the same coupling strength as in Fig. 2(b). It is seen that hole transmission is enhanced by using GaN instead of GaAs. For electron transmission, it is interestingly shown in Fig. 4(c) that Si (100) has two conduction minima (out of six) very close to the K points. To keep symmetry in the unit cell and the simplicity of the tight-binding model, the conduction band minima of Si are set at half period away from the Γ point along the k_y direction, shifted from the blue solid line (expected larger transmission) to the dashed line, in Fig. 4(c). Comparing with transmission coefficient through the conduction band of the vertical GaAs-graphene-GaAs heterostructure (upper plot in Fig. 2(b)), the transmission through the Si conduction valley near K with the same coupling strength is greatly improved by about two orders of magnitude, shown in Fig. 4(d).

IV. Conclusion

We have gained physical insights on transport across vertical semiconductor-graphene-semiconductor heterostructures with quantum transport simulations using an atomistic tight-binding Hamiltonian, and a simplified pseudocubic structure for the semiconductor. We have highlighted that the one-atom-thin graphene layer is not simply "transparent". We have shown that the transmission coefficient through the heterostructure is highly dependent on the coupling between graphene and the semiconductor, which also depends on the fabrication process, and on their transmission overlaps in the k-space. We stress that these aspects can represent optimization possibilities for graphene-based vertical heterostructure devices, such as graphene base transistors, and suggestions for further experiments, with alternative materials and process options.

References

[1] K. S. Novoselov *et al.*, "Electric field effect in atomically thin carbon films," *Science*, vol. 306, no. 5696, pp. 666–669, 2004.
[2] Y.-M. Lin *et al.*, "100-GHz transistors from wafer-scale epitaxial graphene," *Science*, vol. 327, no. 5966, p. 662, Feb. 2010.
[3] L. Liao *et al.*, "High-speed graphene transistors with a self-alignednanowire gate," *Nature*, vol. 467, no. 7313, pp. 305–308, Sep. 2010.
[4] Y. Wu *et al.*, "High-frequency, scaled graphene transistors on diamond-like carbon," *Nature*, vol. 472, no. 7341, pp. 74–78, Apr. 2011.
[5] L. Britnell *et al.*, "Field-effect tunneling transistor based on vertical graphene heterostructures," *Science*, vol. 335, no. 6071, pp. 947–950, Feb. 2012.
[6] G. Fiori, S. Bruzzone, and G. Iannaccone, "Very large current modulation in vertical heterostructure graphene/hBN transistors," *IEEE Trans. Electron Devices*, vol. 60, no. 1, pp. 268–273, Jan. 2013.
[7] W. Mehr *et al.*, "Vertical graphene base transistor," *IEEE Electron Device Lett.*, vol. 33, no. 5, pp. 691–693, May 2012.
[8] B. D. Kong *et al.*, "Two dimensional crystal tunneling devices for THz operation," *Appl. Phys. Lett.*, vol. 101, no. 26, p. 263112, Dec. 2012.
[9] H. Yang *et al.*, "Graphene barristor, a triode device with a gate-controlled Schottky barrier," *Science*, vol. 336, no. 6085, pp. 1140–1143, May 2012.
[10] C. Zeng *et al.*, "Vertical graphene-base hot-electron transistor," *Nano Lett.*, vol. 13, no. 6, pp. 2370–2375, May 2013.
[11] S. Vaziri *et al.*, "A graphene-based hot electron transistor," *Nano Lett.*, vol. 13, no. 4, pp. 1435–1439, Mar. 2013.
[12] V. Di Lecce *et al.*, "Graphene base transistors: A simulation study of DC and small-signal operation," *IEEE Trans. Electron Devices*, vol. 60, no. 10, pp. 3584–3591, Oct. 2013.
[13] V. Di Lecce *et al.*, "Graphene-base heterojunction transistor: An attractive device for terahertz operation," *IEEE Trans. Electron Devices*, vol. 60, no. 12, pp. 4263–4268, Dec. 2013.
[14] J.-N. Longchamp *et al.*, "Low-energy electron transmission imaging of clusters on free-standing graphene," *Appl. Phys. Lett.*, vol. 101, no. 11, p. 113117, Sep. 2012.
[15] R. Saito, G. Dresselhaus, and M. S. Dresselhaus, *Physical Properties of Carbon Nanotubes*. London, U.K.: Imperial College Press, 1998.
[16] R. Zhou, L. C. L. Y. Yoon, and Y. Zhuang, "Properties of two-dimensional silicon grown on graphene substrate," *J. Appl. Phys.*, vol. 114, no. 9, p. 093711, 2013.
[17] K. Xu *et al.*, "Direct measurement of Dirac point energy at the graphene/oxide interface," *Nano Lett.*, vol. 13, no. 1, pp. 131–136, 2012.
[18] (2014, Jun.). [Online]. Available: http://www.ioffe.rssi.ru/SVA/NSM/Semicond
[19] G. Fiori and G. Iannaccone, "Multiscale modeling for graphene-based nanoscale transistors," *Proc. IEEE*, vol. 101, no. 7, pp. 1653–1669, Jul. 2013.
[20] G. Fiori and G. Iannaccone. (2014, Jun.). *NanoTCAD ViDES* [Online]. Available: vides.nanotcad.com.